# Dual-channel phase-shifting interferometry for microscopy with second wavelength assistance

**Juanjuan Zheng (郑娟娟)[1,2], Baoli Yao (姚保利)[1*], Romano A. Rupp[3], Tong Ye (叶 彤)[1], Peng Gao (郜 鹏)[1], Junwei Min (闵俊伟)[1], and Rongli Guo (郭荣礼)[1]**

[1]*State Key Laboratory of Transient Optics and Photonics, Xi'an Institute of Optics and Precision Mechanics, Chinese Academy of Sciences, Xi'an 710119, China*

[2]*Graduate University of Chinese Academy of Sciences, Beijing 100049, China*

[3]*Faculty of Physics, University of Vienna, Boltzmanngasse 5, A-1090 Vienna, Austria*

[*]*Corresponding author: yaobl@opt.ac.cn*

Received April 6, 2011; accepted May 28, 2011; posted online August 5, 2011

Dual-channel phase-shifting interferometry for simultaneous phase microscopy is presented. Red and blue light beams are used for microscope illumination. A 45° tilted beamsplitter replicates the object and reference waves in red light together with the object wave in blue light into two parallel beams. The two resulting quadrature phase-shifting interferograms in red light and the object waves in blue light are generated in the two channels. The two interferograms are recorded simultaneously by a color charge-coupled device (CCD) camera, and can be separated via RGB components of the recorded color patterns without crosstalk. As a result, the phase of tested specimen can be retrieved. The feasibility of the proposed method is demonstrated by test performed on a microscopic specimen.

*OCIS codes:* 090.2880, 180.3170, 120.3180, 170.3880.

*doi: 10.3788/COL201210.010901.*

Interferometry is a nondestructive, high-resolution, and whole-field technique for measuring profiles of many types of surfaces, thickness distribution of transparent specimen, and others[1−5]. On-axis interferometry is able to make full use of the sampling power of a charge-coupled device (CCD) camera, thereby capturing finer spatial details of a sample. However, it is not suitable for simultaneous measurement of moving objects or dynamic processes due to the sequential phase-shifting operation required to eliminate zero-order and twin images. Off-axis interferometry is able to perform phase measurement via one carrier-frequency interferogram; however, it relies on the frequency spectra separation of different terms in the interferogram, thereby resulting in higher requirement on the CCD bandwidth.

Two-step phase-shifting interferometry (TSPSI), which reconstructs the complex amplitude of the object wave from only two phase-shifting interferograms, is a tradeoff between acquisition rate and CCD bandwidth requirement. TSPSI can be classified into three schemes. The first scheme is defined as the "standard" TSPSI, where two quadrature-phase-shifting interferograms and two intensity values (i.e., object wave intensity and reference wave intensity) are needed to reconstruct the phase of the specimen[6]. Meng *et al.* proposed a second scheme of the TSPSI, in which two quadrature-phase interferograms and one intensity value of the reference wave are needed to reconstruct the complex amplitude of the object wave[3]. Recently, Liu *et al.* proposed a third scheme of TSPSI[7], in which an iterative method is used to reconstruct the complex amplitude of the object wave from only two quadrature phase-shifted interferograms. The last two TSPSI schemes both require that the reference wave intensity be premeasured and be no less than twice the maximal intensity of object wave. As a consequence, the fringe visibility of the interferograms is lower than that of traditional phase-shifting interferometry (PSI). Shaked *et al.* proposed two-step phase-shifting slightly off-axis interferometry where the direct current (DC) term is successfully suppressed by subtracting one phase-shifting interferogram from the other[8]. This method requires neither former knowledge nor prediction of any of the waves to recover phase information, while simultaneously maintaining high visibility of the interferogram; however, it still requires high CCD bandwidth to record the off-axis interferogram compared with an on-axis PSI. Furthermore, parallel phase-shifting technique, which records multiple phase-shifting interferograms with one exposure, has trigged with interest in simultaneous phase measurement[9−19].

In this letter, a variation of the "standard" TSPSI for simultaneous microscopy with parallel phase-shifting technique is proposed. The parallel phase-shifting unit is constructed with a 45° tilted cube beamsplitter (BS) that splits the object and reference waves into two parallel beams. The obtained two quadrature phase-shifting interferograms (red light) and object wave (blue light) are recorded simultaneously by a color CCD camera. The two red interferograms and the blue object wave can be separated without crosstalk via the RGB components of the CCD. The complex amplitude of the specimen can then be obtained simultaneously together with the premeasured reference wave. Compared with the two-wavelength simultaneous phase microscopy with off-axis configuration[20], the proposed method maintains the real-time measurement ability while having has lower requirement on CCD resolving power due to its on-axis configuration.

The proposed parallel two-step phase-shifting configuration is shown in Fig. 1(a). The input object (O) and reference (R) waves have linear polarizations (i.e., orthogonal (s-polarization) and parallel (p-polarization),

 

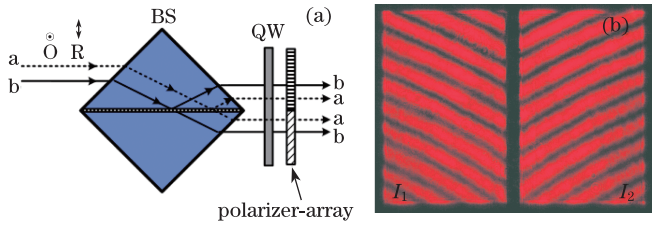


Fig. 1. Dual-channel phase-shifting mechanism. (a) Scheme of the dual-channel phase-shifting configuration. (b) Obtained parallel two phase-shifting interferograms with phase shift of $-\pi/2$.

respectively) to the plane of incidence. These polarizations remain unchanged after refraction and reflection on the nonpolarizing cube BS, and are used to perform polarization phase-shifting processes afterwards. The cube BS is placed in such way that its central semireflecting layer is parallel to the propagation direction of the incident beam. Unlike the single-element interferometer[20−23] where the object and reference waves strike and travel from different sides into the beamsplitter BS, in the proposed configuration, both beams come from the same side. They are split into two parallel copies by transmission and reflection at the central semireflecting layer. The lower beams are those transmitted; thus, they are simply translated replicas of the input object and reference waves. In contrast, the upper beams result from reflection; thus, they are mirror-reversed replicas of the input.

For illustration of the ray trajectory, we have chosen two example rays "a" and "b" in Fig. 1(a). As shown, the distance of the splitting of both beam paths depends on the position where the beam enters (e.g., the splitting of "a" is smaller than that of "b"). This means that the distance between the splitted beams can be adjusted such that it is as close as the physical thickness of the semireflecting layer. In order to obtain the desired phase shift between the object and reference waves of the two split beams, a quarter-wave (QW) plate is employed to transform the two waves to orthogonal circular polarization. A polarizer array is positioned in front of the digital camera for the purpose of performing the phase shifting. The polarizer array is composed of two polarizers with their polarization crossed at an angle of $\pi/4$; both polarizers are located in the paths of the two split beams. According to the analysis on the polarization phase-shifting mechanism proposed by Rodriguez-Zurita[14], a phase shift of $\pi/2$ in the two interferograms can be obtained. In addition, an extra phase shift of $\pi$ will exist between the interferograms. This is because the perpendicularly polarized object wave and reference wave have a phase shift of $\pi$ due to the reflection on the semireflecting layer of the cube beamsplitter BS, as required by symmetry and energy conservation[21]. Thus, the total phase shift between both interferograms will be $3\pi/2$ (or $-\pi/2$) in the CCD plane, as shown in Fig. 1(b).

The experimental setup for parallel dual-channel PSI is shown in Fig. 2. The setup is based on a microscopic Mach-Zehnder interferometer, where microscope objective MO (NA=0.65, $M$=40x) and collimating lens L($f_{\rm L}$=100 mm) are introduced into the object arm to magnify the specimen. A nonpolarized He-Ne laser with wavelength of 632.8 nm (red light) is used to generate the interference pattern for phase microscopy. A vertically linearly polarized continuous wave (CW) argon ion laser with wavelength of 476 nm (blue light) is used as auxiliary light to measure the transmittance distribution of the specimen. The intensities of the red and blue beams are controlled by the variable neutral attenuators $NF_1$ and $NF_2$, respectively. The polarization direction of polarizer $P_1$ has an angle of 45° with respect to the horizontal direction. The cube BS $BS_1$ couples the red and blue beams together and splits them into object and reference waves. In the path of the object wave, both red and blue beams pass through the polarizer $P_3$ and become vertically linearly polarized waves. These waves are expanded by the beam expander $BE_1$, and then illuminate the specimen located in the front focal plane of the microscopic objective MO. After passing through the specimen, the object waves are magnified by the MO and collimated by the lens L. The output object waves become plane waves; the phase curvature brought by the objective is automatically eliminated in the experiment[3]. The polarizer $P_2$ with horizontal polarization is located in the path of the reference wave; thus, the vertically linearly polarized blue beam is completely blocked. The red reference wave is expanded by the beam expander $BE_2$ and reflected by the cube BS $BS_2$; thus, they are directed with the object wave into the dual-channel phase-shifting unit. An aperture is used to restrict the imaging area of the object to fit the field of view of the digital camera. The object waves of two wavelengths and the red light reference wave pass through the dual-channel phase-shifting unit, which is composed of the cube BS $BS_3$, a QW plate, and a polarizer array. Two interferograms with a phase shift of $-\pi/2$ in the red beam are obtained in the two channels of the unit. The two interferograms (red light) and the object wave intensity (blue light) are recorded simultaneously by a color CCD camera with 1 024×768 (pixels) of pixel size 4.65×4.65 ($\mu$m). The red and blue images can be extracted without crosstalk with the aid of the RGB color filter of the CCD sensor.

As shown in Fig. 1(b), the two resulting phase-shifting interferograms have a phase shift of $-\pi/2$, and each is mirror-reversed with respect to the other because the interferogram in the left channel is generated by reflection. After the reversion of the interferogram generated by reflection, the intensity distributions of the two interferograms can be written as

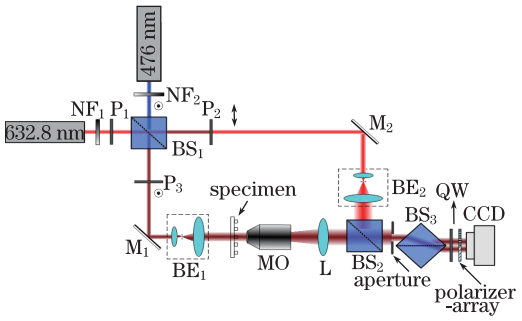


Fig. 2. Experimental setup for dual-channel PSI for microscopy. The double–headed arrow and dots denote the polarization directions.

$$\begin{cases} I_1 = I_{\rm O} + I_{\rm R} + 2\sqrt{I_{\rm O} I_{\rm R}}\cos\varphi \\ I_2 = \gamma_{\rm O} I_{\rm O} + \gamma_{\rm R} I_{\rm R} - 2\sqrt{\gamma_{\rm O}\gamma_{\rm R} I_{\rm O} I_{\rm R}}\sin\varphi \end{cases}, \quad (1)$$

where $I_{\rm O}$ and $I_{\rm R}$ denote the intensity distributions of the object and reference waves in $I_1$; $\varphi$ denotes the phase difference between the two waves; $\gamma_{\rm O}$ and $\gamma_{\rm R}$, respectively, denote the ratios of the intensities of the object and reference waves in $I_2$ with respect to that in $I_1$. Actually, $\gamma_{\rm O}$ and $\gamma_{\rm R}$ depend only on the polarizations of the object and reference waves, rather than on the specimen. Thus, the coefficients $\gamma_{\rm O}$ and $\gamma_{\rm R}$, as well as the intensity of the reference wave, can be measured in advance and used as a calibration constant.

The blue light object waves in both interferograms are denoted with $I_{\rm b1}$ and $I_{\rm b2}$. Linear relations exists for a specimen without chromatic absorption at both wavelengths : $I_{\rm O} = \alpha_1 I_{\rm b1}$ and $\gamma_{\rm O} I_{\rm O} = \alpha_2 I_{\rm b2}$. The coefficients $\alpha_1$ and $\alpha_2$ rely on the wavelength dependence of the CCD color filter and on the beamsplitting ratio of the tilted cube BS. The coefficients can be calibrated by measuring the red and blue object waves in the absence of any specimen, and then calculating the coefficients by $\alpha_1 = I_{\rm O0}/I_{\rm b1}$ and $\alpha_2 = \gamma_{\rm O} I_{\rm O0}/I_{\rm b2}$. Here, $I_{\rm O0}$ and $\gamma_{\rm O} I_{\rm O0}$ denote the object wave intensities for red light in both interferograms, whereas $I_{\rm b1}$ and $I_{\rm b2}$ denote the object waves for blue light in both interferograms measured in the absence of any specimen. Placing $I_{\rm O} = \alpha_1 I_{\rm b1}$ and $\gamma_{\rm O} I_{\rm O} = \alpha_2 I_{\rm b2}$ into Eq. (1), the complex amplitude of the tested object wave can be obtained by

$$O_{\rm r}(x,y) = \frac{I_1 - \alpha_1 I_{\rm b1} - I_{\rm R}}{2\sqrt{\alpha_1 I_{\rm b1} I_{\rm R}}} + {\rm i}\frac{I_2 - \alpha_2 I_{\rm b2} - \gamma_{\rm R} I_{\rm R}}{2\sqrt{\alpha_2 \gamma_{\rm R} I_{\rm b2} I_{\rm R}}}. \quad (2)$$

Using Eq. (2), the complex amplitude distribution of the object wave can be reconstructed.

In order to verify the feasibility of the proposed method, the corresponding experiment was carried out. A rectangular phase step ($70\times 20$ ($\mu$m)) was used as specimen. The phase step was etched into a silica glass plate, and the phase modulation of the phase step is 0.23 (unit: $2\pi$), which corresponds to an optical path difference of 0.23 $\lambda$ ($\lambda$ = 633 nm). The red interferograms and the blue object wave intensity are recorded simultaneously by a color CCD camera, as seen in Fig. 3(a). From the R (red) and B (blue) components of the recorded color hologram, the red interferogram light and the blue object wave intensity are separated, as shown in Figs. 3(b) and (c), respectively. Notably, the red and blue object waves do not perfectly overlap with one another due to the chromatic refraction of the cube BS. To deal with this problem, the domains of the two interferograms and that of the blue object wave are defined accordingly to guarantee that the red object wave is superposed with the blue one.

Using Eq. (2), the complex amplitude distribution of the object wave is reconstructed. After the phase distribution of the setup itself is subtracted, the phase distribution of the phase step is obtained, as shown in Fig. 3(d). To verify the accuracy of the proposed method, the phase along a cut line crossing the phase step is extracted and compared with that obtained by the standard four-step PSI method. As shown in Fig. 3(e), the mean value of the deviation between the phases measured by the mean square (RMS) of the deviation is 0.022 (unit: $2\pi$).

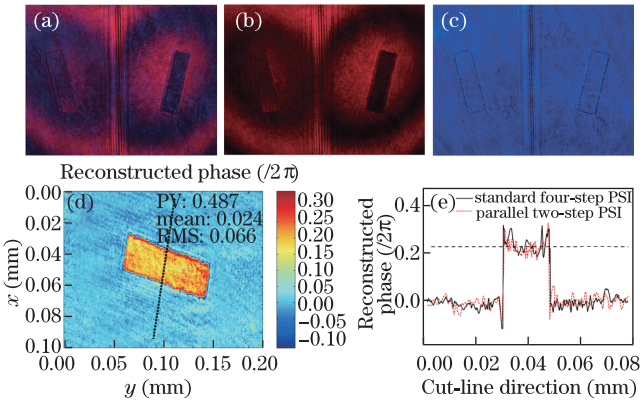


Fig. 3. (Color online) Experimental results for a rectangular phase step. (a) Recorded interferograms from a color CCD camera. (b) Separated dual-channel phase-shifting interferograms of the specimen with phase shift $-\pi/2$ of red light. (c) Separated blue object wave intensity distribution. (d) Reconstructed phase distribution of the rectangular phase step. (e) Phase distribution along the cut-line direction in (d) compared with that obtained with the four-step PSI method.

Such low deviation indicates that the proposed method is consistent with the standard four-step PSI for phase measurement. Furthermore, Fig. 3(e) shows that the average phase modulation of the phase step measured by the proposed method is 0.225 (unit: $2\pi$), which indicates that the measurement accuracy of the proposed method is 0.005 (unit: $2\pi$) when compared with the real value 0.23 (unit: $2\pi$). The accuracy is nearly the same with the standard four-step PSI method. The repeatability of the setup, which is defined as the RMS of the phase difference for two measurements with the same specimen-free setup, is approximately $\lambda/50$. The repeatability of the setup can be improved by using frequency- and output-stabilized lasers or by reducing the exposure time of the CCD camera, as along with the environmental disturbance.

In conclusion, two-color dual-channel PSI for microscopy based on a single-element cube BS has been proposed in this letter. The BS replicates the perpendicularly polarized object and reference waves (red light) into two parallel beams using polarization elements, thereby generating dual-channel phase-shifting interferograms. An additional blue light is used to measure the transmittance of the red object wave and is recorded simultaneously with the red interferograms by a color CCD camera. Both the red interferograms and the blue object waves can be separated without crosstalk because they respond to different RGB channels of the color CCD camera. Thus, the complex amplitude of the object wave can be retrieved. Notably, this method can only be used for specimens with achromatic absorption for the two wavelengths; otherwise, a calibration of the coefficients $\alpha_1$ and $\alpha_2$, which denote the absorption ratios between the red and blue components, respectively, is obligatory.

This work was supported by the National Natural Science Foundation of China (Nos. 61077005 and 10874240) and the Chinese Academy of Sciences/State Administration of Foreign Experts Affairs of China International Partnership Program for Creative Research Teams.

## References


1. J. Schwider, R. Burow, K.-E. Elssner, J. Grzanna, R. Spolaczyk, and K. Merkel, Appl. Opt. **22,** 3421 (1983).
2. F. Charrière, J. Kühn, T. Colomb, F. Montfort, E. Cuche, Y. Emery, K. Weible, P. Marquet, and C. Depeursinge, Appl. Opt. **45,** 829 (2006).
3. X. F. Meng, L. Z. Cai, X. F. Xu, X. L. Yang, X. X. Shen, G. Y. Dong, and Y. R. Wang, Opt. Lett. **31,** 1414 (2006).
4. P. Gao, I. Harder, V. Nercissian, K. Mantel, and B. Yao, Opt. Lett. **35,** 712 (2010).
5. L. Rong, W. Xiao, F. Pan, S. Liu, and R. Li, Chin. Opt. Lett. **8,** 653 (2010).
6. P. Guo and A. Devaney, Opt. Lett. **29,** 857 (2004).
7. J. Liu and T. Poon, Opt. Lett. **34,** 250 (2009).
8. N. T. Shaked, M. T. Rinehart, and A. Wax, Opt. Lett. **34,** 767 (2009).
9. R. Smythe and R. Moore, Opt. Eng. **23,** 361 (1984).
10. M. Novak, J. Millerd, N. Brock, M. North-Morris, J. Hayes, and J. Wyant, Appl. Opt. **44,** 6861 (2005).
11. Y. Awatsuji, T. Tahara, A. Kaneko, T. Koyama, K. Nishio, S. Ura, T. Kubota, and O. Matoba, Appl. Opt. **47,** D183 (2008).
12. T. Kakue, Y. Moritani, K. Ito, Y. Shimozato, Y. Awatsuji, K. Nishio, S. Ura, T. Kubota, and O. Matoba, Opt. Express **18,** 9555 (2010).
13. J. Hahn, H. Kim, Y. Lim, E. Kim, and B. Lee, Chin. Opt. Lett. **7,** 1113 (2009).
14. N. Toto-Arellano, G. Rodriguez-Zurita, C. Meneses-Fabian, and J. Vazquez-Castillo, Opt. Express **16,** 19330 (2008).
15. C. Meneses-Fabian, G. Rodriguez-Zurita, M. Encarnacion-Gutierrez, and N. I. Toto-Arellano, Opt. Commun. **282,** 3063 (2009).
16. N. Shaked, T. Newpher, M. Ehlers, and A. Wax, Appl. Opt. **49,** 2872 (2010).
17. M. Kujawinska and D. W. Robinson, Appl. Opt. **27,** 312 (1988).
18. L. Chen, S. Yeh, A. Tapilouw, and J. Chang, Opt. Commn. **283,** 3376 (2010).
19. B. García, A. Moore, C. Pérez-López, L. Wang, and T. Tschudi, Appl. Opt. **38,** 5944 (1999).
20. M. Rinehart, N. Shaked, N. Jenness, R. Clark, and A. Wax, Opt. Lett. **35,** 2612 (2010).
21. M. Santarsiero and R. Borghi, Opt. Lett. **31,** 861 (2006).
22. J. Ferrari and E. Frins, Opt. Commun. **279,** 235 (2007).
23. Q. Weijuan, Y. Yingjie, C. Choo, and A. Asundi, Opt. Lett. **34,** 1276 (2009).